

## Supporting Information

### **Carbon Dots Hybrid Porous Carbon Nanofibers as Efficient Electrocatalysts for Oxygen Reduction Reaction**

Hongwu Yuan<sup>#,1</sup>, Penghuan Liu<sup>#,1</sup>, Jun Ren<sup>2</sup>, Zhan, Jiang<sup>1</sup>, Xiaohan Wang<sup>\*,1</sup>,  
Haiguang Zhao<sup>\*,1</sup>

<sup>1</sup> College of Textiles and Clothes, State Key Laboratory of Bio-Fibers and Eco-  
Textiles, Qingdao University, No. 308 Ningxia Road, Qingdao 266071, P.R. China

<sup>2</sup> School of Chemical Engineering and Technology, North University of China,  
Taiyuan 030051, P.R. China.

Email: [xh\\_wang@qdu.edu.cn](mailto:xh_wang@qdu.edu.cn); [hgzhao@qdu.edu.cn](mailto:hgzhao@qdu.edu.cn)

#These authors contributed equally to this work

## 1. Characterizations

The morphologies and structures of the various types of fabricated fibers were characterized using field emission scanning electron microscopy (FESEM; Zeiss, Sigma 300). TEM and HRTEM analyses were conducted using a JEOL JEM 2100Plus TEM operating at 200 kV to obtain transmission electron microscopy and high-resolution transmission electron microscopy images. X-ray photoelectron spectroscopy spectra were recorded utilizing a Thermo Scientific K-Alpha XPS spectrometer. Raman spectra were obtained using a LabRAM HR800 (HORLBA JY) instrument. Specific surface area and porosity data were acquired via nitrogen adsorption measurements (Kubo-x1000).

## 2. Figures and tables

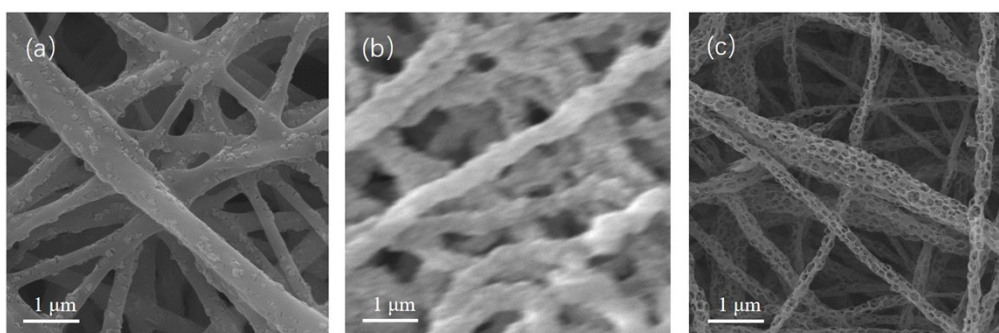


**Figure S1.** SEM images of (a) electrospun nanofibers, (b) oxidized nanofibers, and (c) mesoporous carbon nanofiber membranes

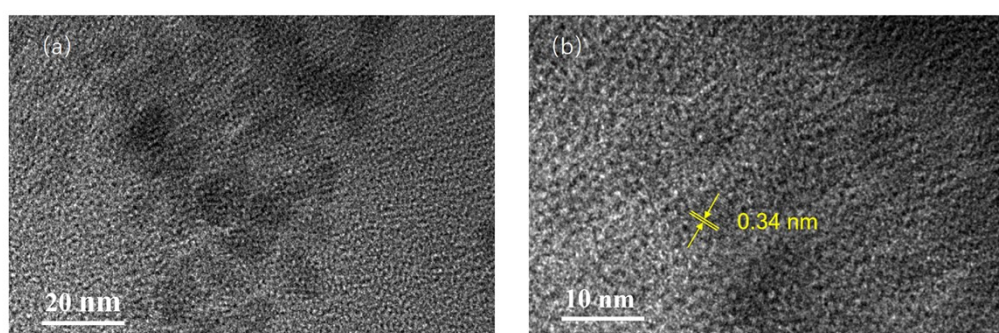


**Figure S2.** (a) TEM image of the C-dots. (b) The corresponding HRTEM image of the C-dots.

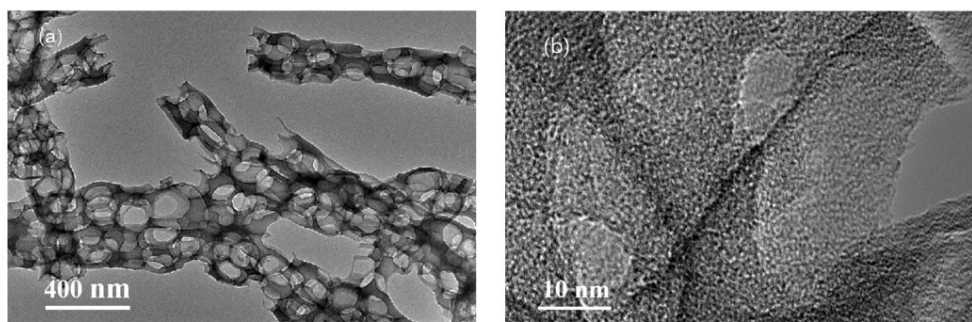


**Figure S3.** (a)TEM image of the PCNFs-900 without adding C-dots. (b)The corresponding HRTEM image of the PCNFs-900 without adding C-dots .

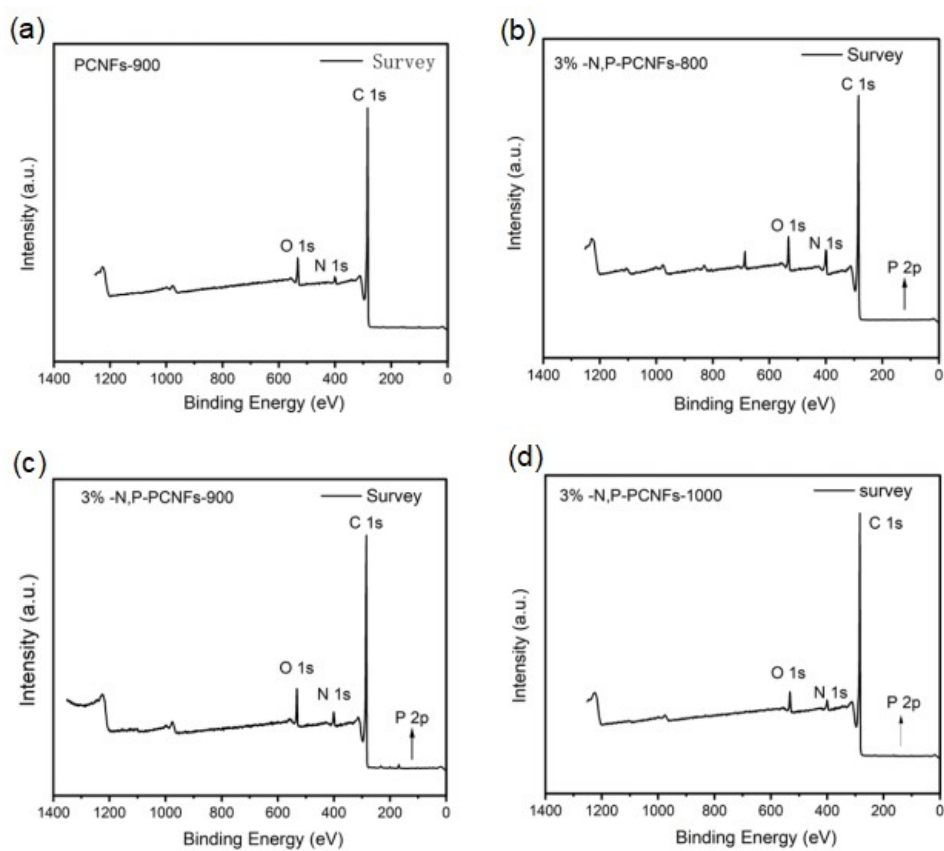


**Figure S4.** XPS survey spectra of the (a) PCNFs-900, (b) N,P-PCNFs-800, (c) N,P-PCNFs-900 and (d) N,P-PCNFs-1000.

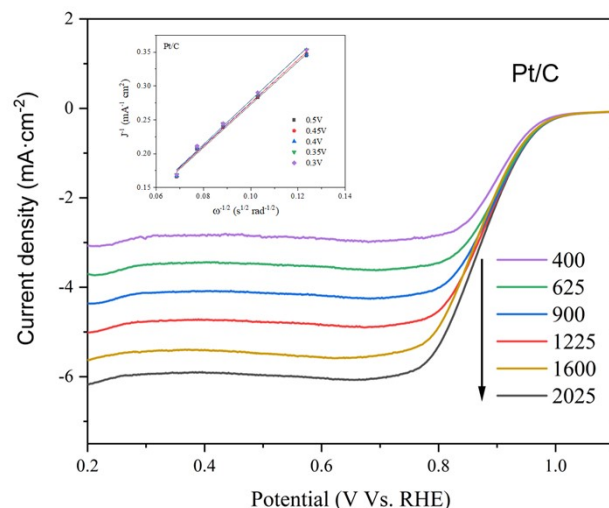


**Figure S5.** LSV curves of the Pt/C at different rotation speeds and the K–L plot at different potentials of Pt/C.

**Table S1** Relative contents of C, N, P, and O in the C-dots and N, P-PCNFs based on XPS measurements.

Sample	Relative contents (%)			
	C	N	O	P
N, P doped C-dots	54.3	8.6	29.7	7.3
3%-N, P-PCNFs-900	89.6	3.8	5.0	1.6
PCNFs-900	92.3	2.5	5.2	0

**Table S2** The atomic ratios of  $N_x/N_{total}$  in the N-P/CNFs [pyridinic nitrogen (N1), pyrrolic nitrogen (N2), graphitic nitrogen (N3), oxidized nitrogen (N0)].

Sample	Relative contents (%)			
	Pyridinic N1	Pyrrolic N2	Graphitic N3	Oxidized N0
3%-N, P-PCNFs-800	38.1	25.3	26.6	10.0
3%-N, P-PCNFs-900	26.5	21.6	37.5	14.4
3%-N, P-PCNFs-1000	17.6	19.6	43.4	19.3
PCNFs-900	28.3	15.9	35.2	20.6

**Table S3** The atomic ratios of P-C and P-O in the 3%-N, P-PCNFs-900.

Sample	Relative contents (%)	
	P-O (133.9)	P-C (132.5)
3%-N, P-PCNFs-900	44.2	55.8

**Table S4.** The onset potential and half-wave potential of electrocatalysts measured in 0.1 M KOH.

Sample	$E_{\text{overpotential}}$ (V vs. RHE)	
	$E_{\text{onset potential}}$	$E_{\text{half-wave potential}}$
PCNFs-900	0.77	0.67
3%-N-PCNFs-900	0.81	0.68
1%-N, P-PCNFs-900	0.83	0.71
2%-N, P-PCNFs-900	0.84	0.70
3%-N, P-PCNFs-800	0.81	0.69
3%-N, P-PCNFs-900	0.88	0.72
3%-N, P-PCNFs-1000	0.80	0.68
Pt/C (20 wt%)	0.92	0.76

**Table S5.**

Sample	$E_{\text{overpotential}}$ (V vs. RHE)		Reference
	$E_{\text{onset potential}}$	$E_{\text{half-wave potential}}$	
NPMC-1000	0.94	0.85	1
N, P-GDs/N-3DG	0.84	0.81	2
P-MC-4	0.86	0.80	3
NPCS-900	0.91	0.83	4
Fe@N-C-12	0.87	0.83	5
Co incorporated into	0.85	0.78	6

---

nitrogen-doped		
carbon nanotubes		
3%-N,P-PCNFs-900	0.88	0.72

---

### Supplementary References

1. J. T. Zhang, Z. H. Zhao, Z. H. Xia, L. M. Dai, A metal-free bifunctional electrocatalyst for oxygen reduction and oxygen evolution reactions, *Nature Nanotechnology*, 2015, 10, 444-452.
2. X. Tong, Mohamed Cherif, G. X. Zhang, X. X. Zhan, J. G. Ma, Ali Almesrati, Francois Vidal, Y. J. Song, Jerome P. Claverie, S. H. Sun, N, P-Codoped Graphene Dots Supported on N-Doped 3D Graphene as Metal-Free Catalysts for Oxygen Reduction, *ACS Applied Materials & Interfaces*, 2021, 13 (26): 30512-30523.
3. H. Zhao, Z. P. Hu, Y. P. Zhu, L. Ge, Z. Y. Yuan, P-doped mesoporous carbons for high-efficiency electrocatalytic oxygen reduction, *Chinese Journal of Catalysis*, 2019, 40, 1366-1374.
4. S. Chen, L. L. Zhao, J. Z. Ma, Y. Q. Wang, L. M. Dai, J. T. Zhang, Edge-Doping Modulation of N, P-Codoped Porous Carbon Spheres for High-Performance Rechargeable Zn-Air Batteries, *Nano Energy*, 2019, 60, 536-544.
5. Y. Ye, H. Li, F. Cai, et al., Two-Dimensional Mesoporous Carbon Doped with Fe-N Active Sites for Efficient Oxygen Reduction, *ACS Catal.*, 2017, 7, 7638-7646.
6. B. Peng, H. Zhang, H. Z. Shao, K. Xu, G. Ni, J. Li, H. Y. Zhua, Costas M. Soukouliscd, Chemical intuition for high thermoelectric performance in monolayer black phosphorus,  $\alpha$ -arsenene and aW-antimonene, *J. Mater. Chem. A: Mater. Energy Sustain.*, 2018, 6, 3386-3390.